RSC Advances

PAPER

View Article Online
View Journal | View Issue

Cite this: *RSC Adv.*, 2017, **7**, 43334

Thermo-oxidative ageing effect on mechanical properties and morphology of short fibre reinforced polyamide composites – comparison of carbon and glass fibres†

Lin Sang,[a] Chuo Wang,[a] Yukai Wang[a] and Zhiyong Wei *[b]

The present paper examined the thermo-oxidative ageing behavior of short carbon fibre reinforced polyamide 6 composites (CF/PA6), in comparison with commercial glass reinforced composites (Ultramid® B3WG7). The mechanical results revealed that the tensile strength of CF/PA6 composites (retention above 90%) was well maintained, while the notched Izod impact strength of both CF/PA6 and Ultramid® B3WG7 were continuously decreased during the ageing process. Annealing effects on PA6 and chain arrangement were found in the initial ageing stage, and a better thermal stability of CF/PA6 compared with the Ultramid® B3WG7 sample was observed from the TGA curves as the ageing time was prolonged. A noticeable color transition from white to black was observed in Ultramid® B3WG7 samples when the increasing ageing temperature. The ageing process also resulted in topography damage with matrix cracks and fibre/matrix interfacial debonding due to chain scission, oxidization and formation of chromophoric groups of polyamide molecules, which was illustrated by scanning electron microscopy (SEM) and Fourier transform infrared (FTIR) spectroscopy. Furthermore, metallographs of polished cross-sections of Ultramid® B3WG7 demonstrated the evolution of an oxidized layer of the composites at increased ageing temperatures for prolonged ageing time, which was ascribed to the contribution of mechanical changes that play an important role at high ageing temperatures.

Received 18th July 2017
Accepted 2nd September 2017

DOI: 10.1039/c7ra07884f

rsc.li/rsc-advances

1. Introduction

In recent years, short fibre reinforced thermoplastics (S-FRTP) have attracted much attention for engineering applications owing to their particular properties of high performance, good processability, economic cost, light weight and potential recyclability.[1–3] Polyamide (PA) is a general engineering thermoplastic resin with excellent performance and heat resistance.[4–8] Short fibre reinforced polyamide (PA6 and PA66) composites have been largely applied in the automotive industry such as semi-structural components and some interior accessories.[9–13] Especially, there has recently been a strong demand in the use of moulded short fibre reinforced polyamide composites that serve as divided manifold, front-end modules and other under-the-hood applications.[14,15] These applications place stringent requirements on short fibre reinforced polyamide composites in terms of dimensional stability, mechanical properties and chemical resistance. Once these composites are exposed to high temperatures for a prolonged period, they become sensitive and vulnerable to factors including radiation, moisture, heat or light.[16–19] Hence, investigations in the mechanical properties and understanding in ageing behavior of fibre reinforced polyamide composites under high temperatures (*i.e.* 150 °C, or even 180–200 °C) is of significant importance for long-term service of PA-based composites.

Thermo-oxidative ageing, an integrated effect of heat and oxygen, is one of main ageing forms for composite materials. Polyamide 6 (PA6) is generally synthesized by the hydrolytic polycondensation of caprolactam monomer and a monofunctional acid, containing repeated amide groups (–CONH–) in the backbone of polymer, which makes the polymer more sensitive to oxidation.[20] High temperatures are known to accelerate polymer oxidation, and the oxygen leads to the auto-oxidation scission of the main chain of polymer.[21] Based on general thermo-oxidative path of aliphatic polyamide,[22,23] degradation of polyamide is predominantly began through the abstraction of a hydrogen atom of the methylene groups adjacent to the nitrogen of amide group –CONH–CH_2–, accompanied by formation of some sensitizers, *i.e.* carbonyl, chromophoric groups or peroxides as oxidation prolonged.[24,25]

In previous publications, research on the thermo-oxidative ageing effect on mechanical properties of glass fibre (GF)

[a]*School of Automotive Engineering, State Key Laboratory of Structural Analysis for Industrial Equipment, Dalian University of Technology, Dalian 116024, China*
[b]*Department of Polymer Science and Materials, School of Chemical Engineering, Dalian University of Technology, Dalian 116024, China. E-mail: zywei@dlut.edu.cn*

† Electronic supplementary information (ESI) available. See DOI: 10.1039/c7ra07884f

reinforced polyamide composites were studied.[26–28] Song *et al.* investigated thermal-oxidative ageing effects on the thermal and dynamic mechanical properties of long glass fibre (LGF) reinforced polyamide 10T composites.[26] Zuo *et al.*[27] studied long-term thermo-oxidative ageing on the flammability and degradation kinetics of PA6/LGF composites which was aged at 160 °C. As increasing attention on CF applied in automotive industry, it is important to evaluate ageing behavior of CF reinforced PA composites. Furthermore, limited studies focused on the relationship between morphology and mechanical performance of short fibre reinforced composites (especially for carbon fibre) under long-term thermo-oxidative ageing condition. Therefore, the evolution of oxidized zones and mechanical properties during thermo-oxidative process is of great necessity of seeking internal ageing mechanism of carbon fibre reinforced polyamide composites.

In the current study, we report the long-term thermo-oxidative ageing effect on the mechanical properties and morphology of short carbon fibre reinforced polyamide composites from both macro and micro view. Commercial glass fibre reinforced PA6 composites are set as controls for comparison. These two kinds of composites are subjected to oven ageing at different times at 90, 130, 150 and 180 °C, respectively. Changes in mechanical properties, thermal stability, color transition, surface microstructure and oxidized layer are recorded and analyzed, which are of prime significance in gaining insight on long-term ageing behavior of carbon fibre reinforced PA6 composites.

2. Experimental

2.1 Materials

Polyamide 6 (commercial grade: Ultramid B3) was supplied by BASF Co., Ld. The carbon fibre (CF) tow (commercial grade: HTS40-6k) was provided by Toho Tenax Co., Ltd. The continuous carbon fibre (HST40-6k, TOHO, Japan) possesses the following characteristics: their density is 1.77 g cm^{-3}, and their tensile strength and tensile modulus is 4.4 GPa and 230 GPa, respectively. Glass fibre reinforced PA6 composites with 35% weight fibre content were supplied from BASF Co., Ltd and commercially graded as Ultramid® B3WG7. The saline agent 3-aminopropyltriethoxy silane coupling agent (KH550, NH_2CH_2-$CH_2CH_2Si(OC_2H_5)_3$, 97% purity), acetone (99.5% purity), alcohol (95% purity) were purchased from Tianjin FuYu chemical co., LTD.

2.2 Preparation of CF20/PA6 and Ultramid® B3WG7 composites

The silane treatment of CF was according to our previous work.[29] PA6 was dried at 100 °C for 8 h in an oven to remove moisture before blending. The silane-treated carbon fibre reinforced PA6 composites were compounding in a twin-screw extruder (SHJ20-X40, $L/D = 40$, $D = 40$ mm, Nanjing Giant Machinery Co., Ltd. China). PA6 was fed from the hopper, and the continuous carbon fibres were automatically fed through the fibre feeding port by rotation of the screw. A continuous strand consist of sheared CF and PA6 matrix were achieved *via* extruding, with ramping temperature profile from feeding zone to die as 265, 270, 275, 270, and 265 °C, respectively. The melting extrudates was cooled in a water bath and then chopped into pellets at a length of 6 mm. The weight fraction of CF was kept at 20 wt% and coded with CF/PA6. The dried granules were molded using an injection molding machine (XTK 1200, Xiatian General Machinery, Ningbo, China). Ultramid® B3WG7, commercial composites with 35 wt% glass fibres were set as control samples.

2.3 Thermo-oxidative ageing

CF/PA6 and the contrast Ultramid® B3WG7 composites were subjected to thermo-oxidative ageing in air-circulating ovens (±1 °C) at 90, 130, 150 and 180 °C up to 1600 h, respectively. The aged samples were removed at regular time intervals and stored at 25 ± 3 °C for at least 24 h prior to testing.

2.4 Characterization

Tensile tests were carried out according to ASTM D-638 using a universal tester (Sans UTM5105X, Shenzhen). The tensile speed was set to 5 mm min^{-1}. Notched Izod impact strength was measured according to ASTM D-256 standard by XQZ-II impact tester (JJ-Test, Chengde, Hebei, China) equipped with a pendulum of 2.75 J. The notch was 2.5 mm and the angular radium was 0.25 mm. The geometry of the mechanical specimen was shown in Fig. 1. All the tests were performed at a constant temperature of 25 °C, and each data point was the average from five specimens.

Dynamic mechanical analysis (DMA) was studied with a Q800 analyzer (TA Instruments) at a heating rate of 3 °C min^{-1} with the frequency of 1 Hz. The temperature was ranged from room temperature to 200 °C and the amplitude was set 10 μm in the bending mold. The dimension of the test specimens was 40 × 10 × 4 mm^3 (length × width × thickness). Storage modulus (E'), loss modulus (E'') and tan δ were determined as a function of temperature.

The thermal stability of composites was investigated by a thermogravimetric analyzer (NETZSCH, TG 209) under nitrogen atmosphere at a purge rate of 100 ml min^{-1}. About 10 mg of each sample were heated from 50 °C to 600 °C at heating rate of 10 °C min^{-1}.

Scanning electron microscopy (SEM) images were captured by scanning electron microscope (SEM, QUANTA 450, FEI), at an accelerating voltage of 20 kV under high vacuum. The surfaces and tensile fractured morphology of both aged and unaged samples were made electrically conductive by sputter coating with a gold layer before examination.

Attenuated total reflectance-Fourier transform infrared spectroscopy (ATR-FTIR, Nicolet iN10, Thermo Fisher Scientific) were used to compare the variation in functional groups of unaged and aged materials. The analysis conditions were 32 scans, at a range of 4000–600 cm^{-1} and 4 cm^{-1} resolution.

The oxidation front of composite samples was observed using microscopic method. A 20 mm long piece cut from the specimen and embedded in a potting compound. The

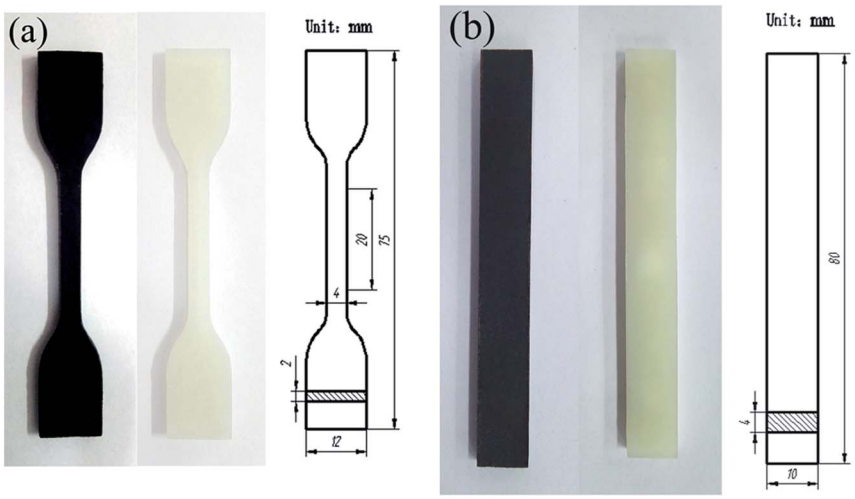

Fig. 1 Geometry of the mechanical specimen (a) tensile test and (b) impact test.

cross-sectional area were polished using sand papers (P400, P1200, P2000) and afterwards polished with a 1 μm diamond suspension. Then the micrographs were obtained by metalloscope (MEF4, Beijing Suohong Sunny Technology Center) after polishing of cross-sections.

3. Results and discussions

3.1 Mechanical properties

The mechanical properties of CF/PA6 and Ultramid® B3WG7 with different thermo-oxidative ageing time were given in terms of tensile strength and notched impact strength. As shown in Fig. 2(a), the average tensile strength of initial CF/PA6 specimen was 152.63 MPa with the standard deviation of 3.33 MPa (152.63 ± 3.33 MPa). When ageing at 90 °C, the tensile strength of CF/PA6 specimens was 171.75 ± 3.83 MPa at 24 h, 185.63 ± 4.28 MPa at 200 h, 193.04 ± 2.27 MPa at 400 h, 177.88 ± 4.53 MPa at 800 h, and 160.75 ± 4.94 at 1600 h. It is interesting to find that the variation tendency of tensile strength of CF/PA6 composites was similar to that at 130, 150 and 180 °C, which increased in the initial ageing time, and then slowly decreased as ageing time increased. Fig. 2(b) presented the tensile strength retention (*i.e.* the tensile strength of aged specimen over the tensile strength of unaged specimen) of CF/PA6. For ageing temperature at 90 °C, the retention of tensile strength was found to keep an increase up to 400 h and then gradually decreased afterward. However, the turning point of retention of the tensile strength was shortened to 200 h at ageing temperature of 150 °C, and further shortened to only 24 h at harsh temperature of 180 °C. When ageing at 90 °C and 130 °C, the retention of the tensile strength was remained above the initial tensile strength until the test ended (up to 1600 h). On the other hand, the tensile strength retention of CF/PA6 specimens was 98% and 91.6% after 1600 h in air-circulating oven at 150 °C and 180 °C, suggesting the tensile strength of CF/PA6 was well-reserved at high ageing temperatures.

Fig. 2(c and d) presented the variation of tensile strength and retention percentage of Ultramid® B3WG7 specimens. The change trend of tensile strength for Ultramid® B3WG7 specimens was analogous to CF/PA6 composites at four different ageing temperatures. However, the reduction in tensile strength was more obvious in Ultramid® B3WG7 specimens. As shown in Fig. 2(c), the initial tensile strength of control glass fibre reinforced composite specimens was 127.88 ± 2.88 MPa. After aged for 1600 h, the tensile strength was 139.38 ± 6.14 MPa at 90 °C, 110.50 ± 3.91 MPa at 130 °C, 105.22 ± 7.12 MPa at 150 °C and 96.75 ± 6.14 MPa at 180 °C, respectively. The results revealed that the retention of tensile strength was well retained at ageing temperature of 90 °C, and gradually decreased as increasing ageing temperatures. For example, after aged for 1600 h at 180 °C, the retention tensile strength of Ultramid® B3WG7 specimens dropped to 75.7%, whereas a high retention strength above 90% in CF/PA6 were maintained, suggesting a better stabilizing effect of carbon fibre than that of glass fibre during the long-term thermo-oxidative ageing.

Fig. 3 showed the typical SEM images of tensile fracture surfaces of CF/PA6 and Ultramid® B3WG7 specimens after they were subjected to varying thermo-oxidative temperatures (90, 130, 150 and 180 °C) for 1600 h. Before thermo-oxidative ageing, the fracture of unaged specimens mostly occurred in the matrix phase rather than in the interface between fibres and PA6 resins. Both carbon and glass fibres were well coated with a certain amount of PA6 resin. As is known, the fibre/matrix interface was a major parameter influencing the final properties of the composite material which were strongly interlinked to the ability to transfer across the interfacial region.[30] Thus, the residue PA6 on fibre surface implied that a high level of interface adhesion was achieved for the unaged CF/PA6 and Ultramid® B3WG7 specimens. After thermo-oxidative conditioned for 1600 h, the interfacial debonds were not clearly evident in CF/PA6 specimens, and only a few voids in the fracture surface due to the pullout of fibres were observed, suggesting a maintained interfacial bonding between PA6 and carbon fibres.

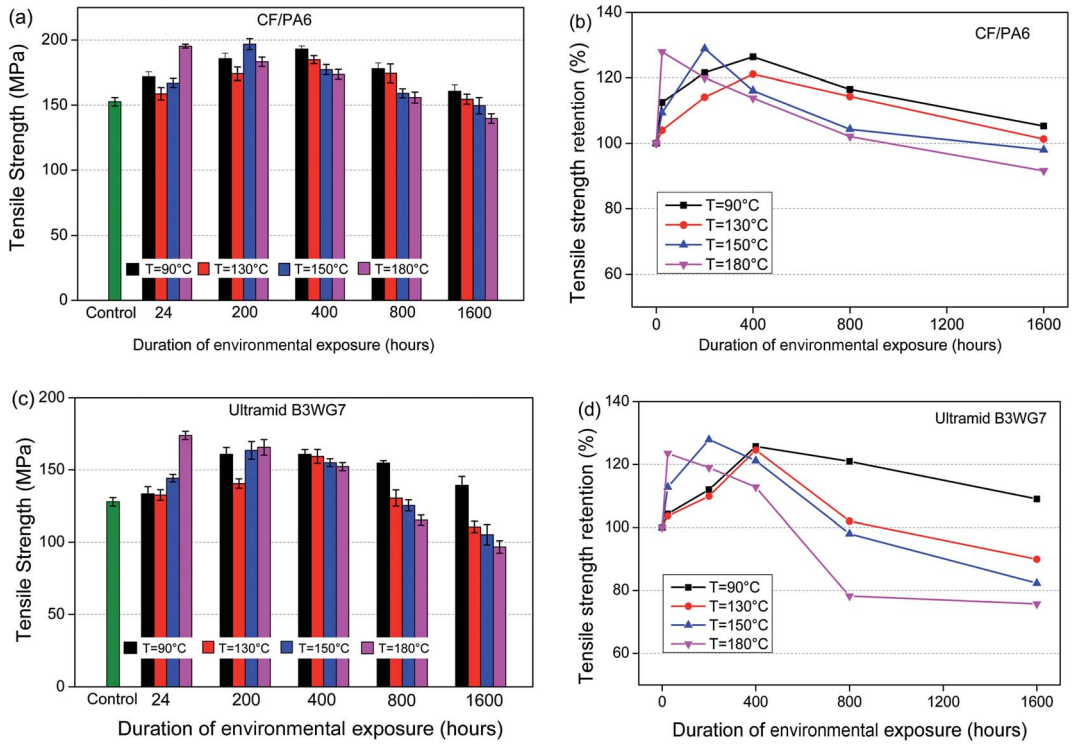

Fig. 2 Effect of different ageing temperature on (a) tensile strength of CF/PA specimen, (b) tensile strength retention of CF/PA specimen, (c) tensile strength of Ultramid® B3WG7 specimen and (d) tensile strength retention of Ultramid® B3WG7 specimen.

Therefore, the strong interface may greatly contribute to a well-retention of tensile strength.[31] On the other hand, the attack of the fibre/matrix interface became obvious in Ultramid® B3WG7 specimens, especially at high ageing temperature of 150 and 180 °C. Also, the PA6 resin became brittle and cracked due to the decomposition of PA6 chains. Consequently, load transfer across the fibre/matrix interface was limited, and interfacial failure and the pull-out fibres took places at these weak interfacial zones, resulting in a reduced tensile strength of Ultramid® B3WG7 samples.

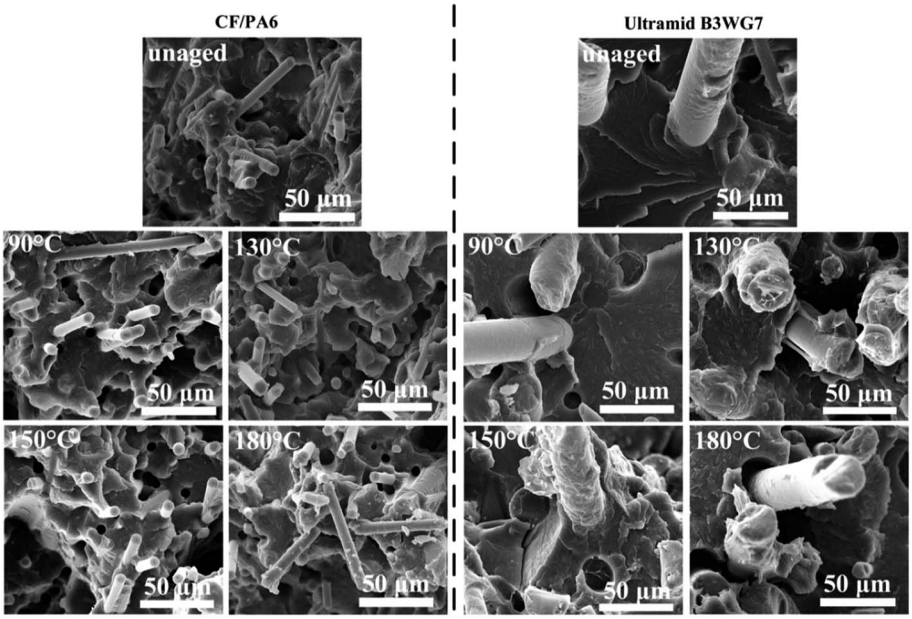

Fig. 3 Scanning electronic micrographs of the tensile fractured surface of CF/PA6 and Ultramid® B3WG7 specimens aged at varying temperatures up to 1600 h.

The variation tendency of notched impact strength of CF/PA6 and Ultramid® B3WG7 specimens was different from that of tensile strength. As shown in Fig. 4, it is found that the notched impact strength continuously decreased to a certain degree during the whole ageing process. For CF/PA6 specimens, the notched impact strength decreased 25.3%, 27.2%, 34.4% and 39.3% after 1600 h of ageing at 90, 130, 150 and 180 °C, respectively. On the other hand, the notched impact strength of Ultramid® B3WG7 specimen decreased more seriously, with a decrease in 41.3% after 1600 h ageing time at a temperature of 180 °C.

3.2 Dynamic mechanical analysis

In the process of thermo-oxidative ageing, the change of modulus and glass transition temperature (T_g) was attributed to the interactions within the molecular chains in the amorphous phase.[32,33] In Fig. 5, the storage modulus (E'), loss modulus (E'') and damping factor (tan δ) values for CF/PA6 and Ultramid® B3WG7 specimens aged at 180 °C were recorded as a function of ageing temperature. In the temperature range of 40–80 °C close to the glassy region, the E' values of CF/PA6 and Ultramid® B3WG7 specimens decreased remarkably and its values became increased in the aged samples in contrast with the unaged ones.

The glass transition temperature (T_g) of composites is always taken by the maximum of tan δ, which implied a relaxation process and involved the extent of the mobility of small groups and the macromolecular chain segments. For CF/PA6 and Ultramid® B3WG7 specimens aged for 400 h, the tan δ shifted to higher temperatures and an increase in T_g (40 °C → 65 °C) were found in comparison with the unaged samples. The increase in T_g was led by the molecular crosslinking reaction during the primary ageing stage, as also observed in previous studies. A reduced E'' values for these two composites was also observed, signifying the crosslinking restricted the mobility of the molecular chain, as also reported from previous literatures.[34,35] The thermo-oxidative exposure temperature exhibited an annealing effect for PA6 matrix during the primary ageing stage, which may explained the initial increase in tensile strength of both CF/PA6 and Ultramid® B3WG7 specimens. As ageing period prolonged to 1600 h, both the peak area of loss modulus and peak intensity of tan δ_{max} were decreased, which implied that the restriction mobility of the molecules and the damping properties. The difficult chain relaxation might be caused by a combination with crosslinking of molecules, thermal-embrittlement and oxidative-embrittlement.[21]

3.3 Thermal stability

TGA was used to compare the thermal stability of CF/PA6 and Ultramid® B3WG7 during thermo-oxidative process. TGA curves of surface samples of these two composites with different ageing time at 180 °C were exhibited in Fig. 6, and the corresponding parameters ($T_{d5\%}$ defined as the onset decomposition temperature at weight loss of 5%, and T_{dmax} as the maximum decomposition rate temperature) were presented in Table 1. The TGA and DTG curve of neat PA6 was illustrated in ESI (Fig. S1†). As shown in these profiles, it can be seen that the onset decomposition temperature of pristine PA6 was 398.0 °C, and then increased to 401.7 °C for CF/PA6 and 399.0 °C with the addition of carbon fibre and glass fibre, respectively. The same situation also went for T_{dmax} of the composites. As already reported,[36,37] the incorporation of reinforcing fibres could improve the thermal stability of the matrix, which was attributed to a physical barrier effect of fibre.

From 0 h to 400 h ageing, the TGA curves for CF/PA6 composites exhibited similar profiles. As the ageing time reached to 1600 h, a slight decrease in $T_{d5\%}$ and T_{dmax} values (~17–20 °C) was observed, exhibiting a relatively excellent thermal stability during long-term and high temperature ageing condition. On the other hand, for the Ultramid® B3WG7 samples, the TGA curve shifted to lower temperature as ageing time prolonged. In detail, the $T_{d5\%}$ considerably declined from 399.0 °C to 350.3 °C aged for 1600 h, while T_{dmax} fells from 467.2 °C (unaged) to 443.9 °C at the end of thermo-oxidative ageing. Meanwhile, it is noticeable found that the degradation residues of Ultramid® B3WG7 have a slight increase with ageing time proceeded. For unaged sample, the weight residue was finally maintained at 35.2%, with equal fibre content as the supplier provided. After aged for 400 h and 1600 h, the weight residue was increased to 36.6% and 37.4% respectively. This might be attributed to the escape of volatile-degraded products from sample surface and therefore decreased the content of PA6 resin in Ultramid® B3WG7 composites. For fibre reinforced PA6 composites, thermal and oxidative reaction may cause the breakage of PA6 and fibre/matrix debonding, inducing

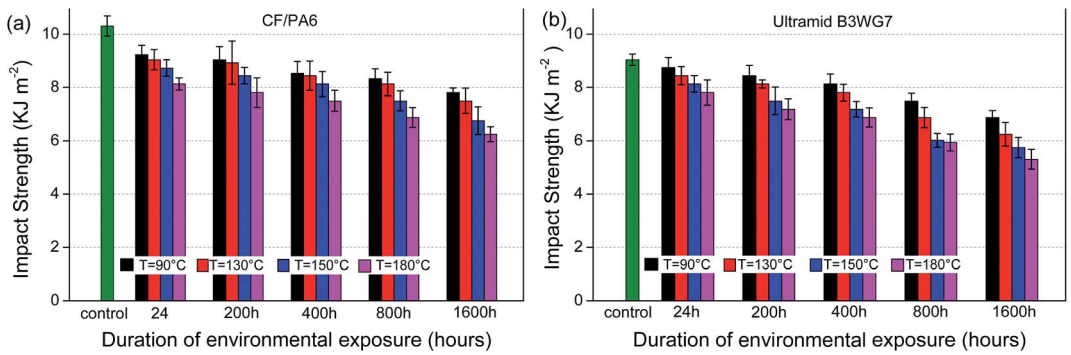

Fig. 4 Effect of different ageing temperature on impact strength of (a) CF/PA6 specimens, (b) Ultramid® B3WG7 specimens.

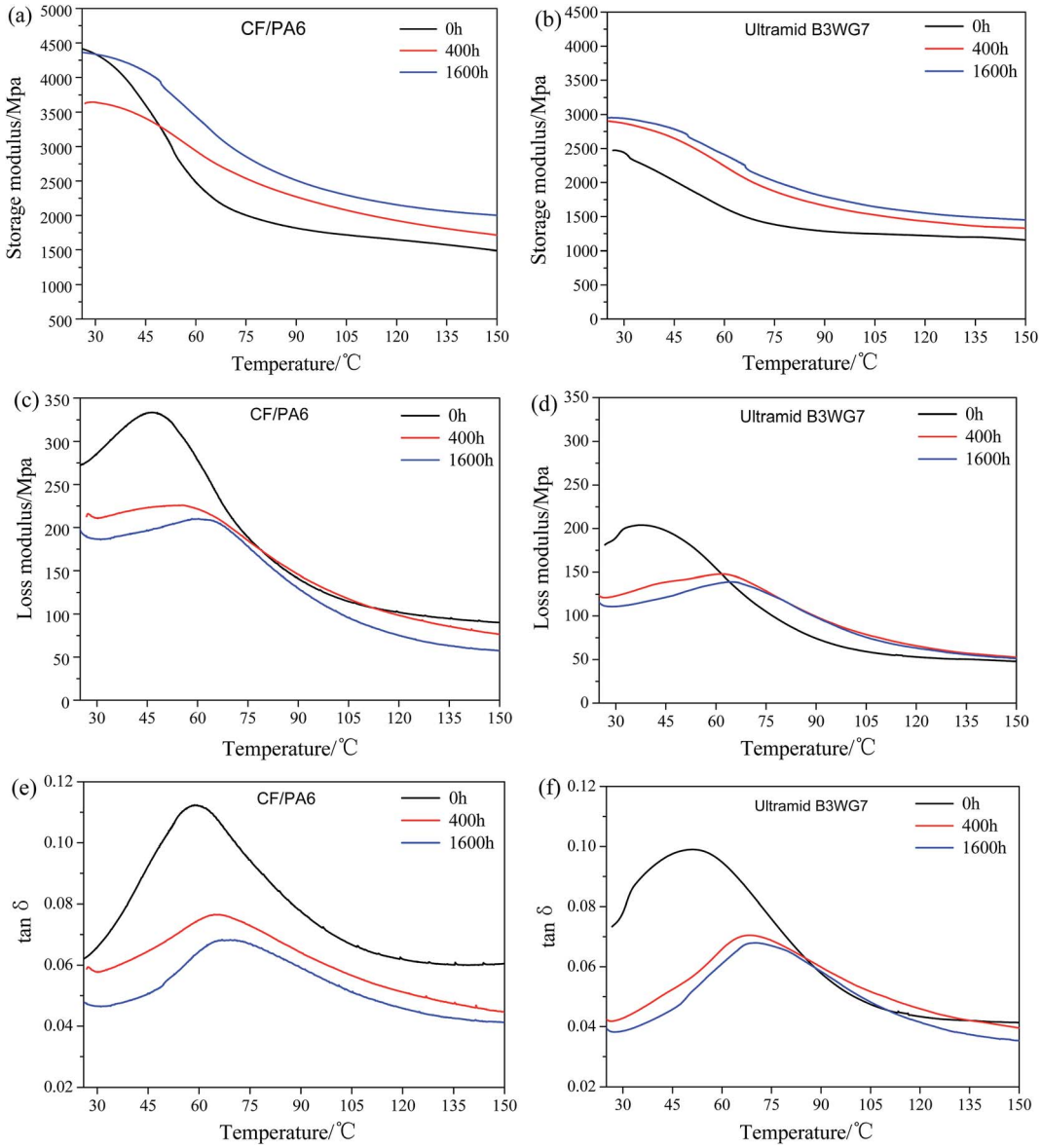

Fig. 5 DMA spectra of CF/PA6 and Ultramid® B3WG7 samples as a function of the ageing time at 180 °C (a and b) storage modulus, (c and d) loss modulus, and (e and f) tan δ.

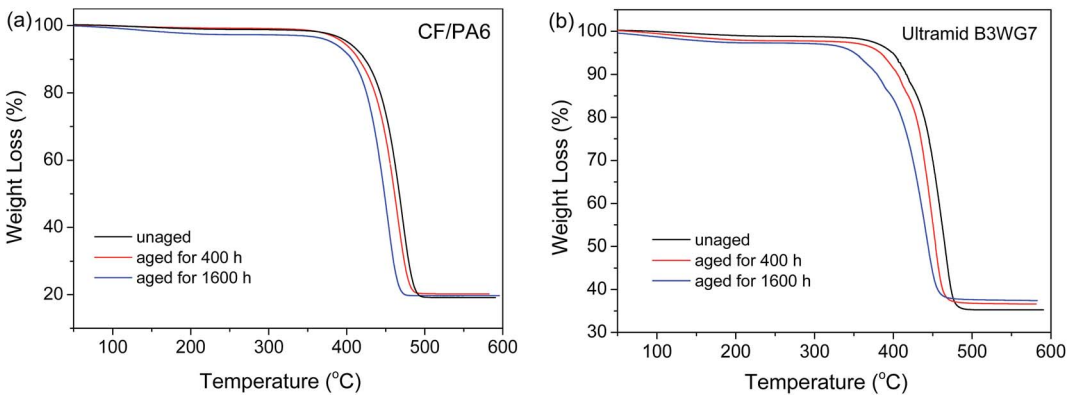

Fig. 6 TGA curves of (a) CF/PA6 and (b) Ultramid® B3WG7 samples as a function of the ageing time at 180 °C.

Table 1 The TGA data of unaged and aged CF/PA6 and Ultramid® B3WG7 samples

	$T_{d5\%}$ (°C)			T_{dmax} (°C)		
Samples	Unaged	400 h	1600 h	Unaged	400 h	1600 h
CF/PA6	401.7	395.2	381.2	471.7	465.0	454.7
Ultramid® B3WG7	399.0	383.4	350.3	467.2	449.4	443.9

a reduction of thermal stability. As illustrated in TGA curves, it can be concluded that CF/PA6 composites maintained better thermal stability in comparison with commercial glass fibre reinforced composites during long-term thermo-oxidative ageing under high temperature. This might be explained by the well-maintained interfacial bonding between carbon fibre and PA6 matrix, as discussed in the next sections concerning surface topography.

3.4 Color transition and chemical analysis

Color change is the easiest noticeable property change of the aged specimens. Thus, evidence of chemical ageing was easily observed by the discoloration of Ultramid® B3WG7 specimens throughout the ageing process. Since the color transition of black CF/PA6 composites were hard to observe, hence, digital images of the Ultramid® B3WG7 specimens for different ageing times at 90, 130, 150 and 180 °C were shown in Fig. 7. It can be observed that the color transition was greatly dependent on the ageing temperatures. When exposed to low-temperature ageing condition, surface color did not change greatly during the whole ageing period. However, surface color changed significantly at increasing ageing temperatures, that is, from white to yellow, dark brown and finally to black. This color change could be directly related to oxidation reaction of PA6 resin. Previous studies have demonstrated that the color change was generally limited to an external layer of composites.[38,39]

The FTIR spectra were used to find out the decomposition of PA6 resin and the reason for the discoloration of CF/PA6 and Ultramid® B3WG7 specimens. The representative FTIR spectra of unaged and aged composites were obtained at surface on the side of CF/PA6 and Ultramid® B3WG7 specimens at varying ageing temperatures for a period of 1600 h. As presented in Fig. 8, for unaged samples, it was observed that the characteristic absorption peaks of hydrogen-bonded NH stretching (3295 cm^{-1} and 3074 cm^{-1}), amide I (1627 cm^{-1}), amide II

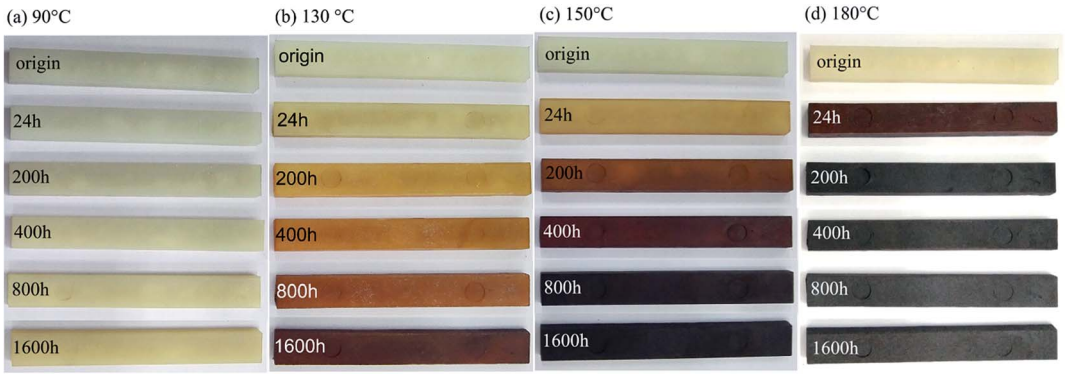

Fig. 7 Digital photos of colour change of Ultramid® B3WG7 specimen as a function of the ageing time at different ageing temperatures (a) 90 °C, (b) 130 °C, (c) 150 °C and (d) 180 °C.

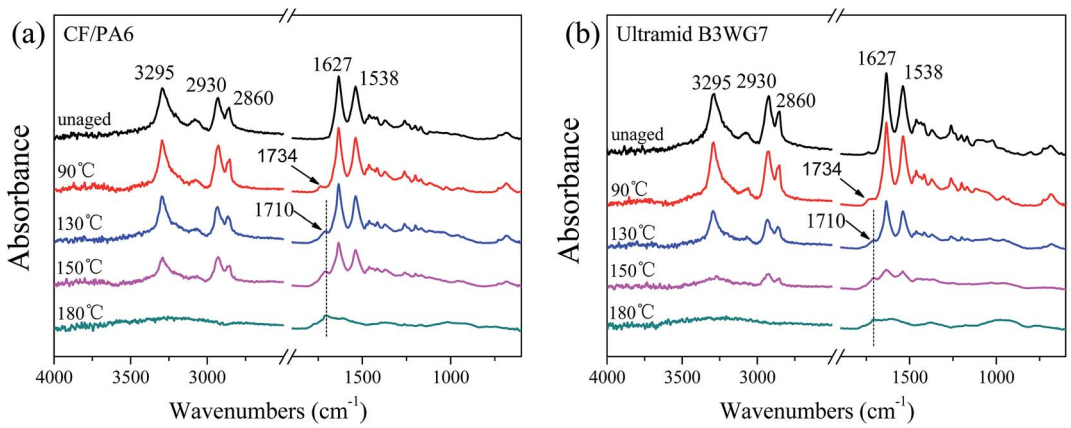

Fig. 8 ATR-FTIR spectra recorded on the surface of the aged samples as a function of ageing temperature after thermo-oxidative for 1600 h (a) CF/PA6 and (b) Ultramid® B3WG7 specimens.

(1538 cm^{-1}) and asymmetric and symmetric CH_2 stretching (2930 cm^{-1} and 2860 cm^{-1}) peaks were belonged to PA6 resin, which was sharp and distinct. With increasing ageing temperatures, the characteristic bands of PA6 were eventually diminished and even disappeared for both CF/PA6 and Ultramid® B3WG7 composites, suggesting that the PA6 molecular chain on composite surface may experience accelerated oxidation reaction at elevated temperatures. Specially, the attenuation of absorption peaks of Ultramid® B3WG7 was more serious than that of CF/PA6 composites at the ageing temperature of 150 °C. In this case, carbon fibre could efficiently block the diffusion of oxygen and further protect the materials from further oxidation.

On the other hand, some new absorption bands at 1710 cm^{-1} and 1734 cm^{-1} were detectable in the surface of aged specimens during ageing process. For the composites aged at 90 °C, the peak at 1734 cm^{-1} was related to the presence of cyclopentanone derivatives. With increasing ageing temperatures, the peak shifted to 1710 cm^{-1} and became evident, which was corresponded to the formation of carbonyls (free C=O) originating from ketone, aldehyde, ester or acid degraded products, which indicated thermo-oxidative degradation of polyamide 6 on sample surface.[40] The chemical species formed during thermo-oxidative ageing, free C=O was inferred as α-keto carboxyl with chromophore structure,[41] which could explain the phenomenon of the color change of composites after 1600 h ageing period. On high-temperature processing (180 °C), the characteristic peaks of PA6 disappeared and newly formed peak at 1710 cm^{-1} were found in the first ageing 400 h. As ageing prolonged, the characteristic peak of carbonyl groups kept unchanged (as presented in ESI, Fig. S2†), indicating that no significant degradation took places until the end of thermo-oxidative ageing.

Fig. 9 showed the surface photomicrograph of CF/PA6 and Ultramid® B3WG7 samples after aged at 180 °C for 400 h and 1600 h compared to the unaged ones, respectively. A relatively smooth and no damage surface were observed in the unaged composites. After aged for 400 h, the embedded fibres became evident, and PA6 resin covered and adhered on carbon and glass fibre surface. After CF/PA6 samples were subjected to thermo-oxidative ageing for a prolonged time (1600 h), some micro-cracks appeared paralleled to the dispersed carbon fibres, and there is PA6 sheathing layer covering on carbon fibre. In contrast, sharp micro-cracks and serious damage of PA6 matrix were clearly observed around glass fibres, which were corresponded to the decreased fibre/matrix interface zone. Also, the glass fibres were mainly exposed on the material's surfaces, probably caused by the rupture of PA6 molecular chain, and thus low-molecular-weight products were volatilized during thermo-oxidative ageing. From the SEM images, it can be revealed that the micro-cracks were appeared along the fibres greater than occurrence in the transverse direction.[42]

Fig. 10 showed the surface microstructure of CF/PA6 and Ultramid® B3WG7 specimens aged for 1600 h at varying ageing temperatures. It can be seen that surface damage of both two composites was more prone to be suffered at high temperature. In comparison with CF/PA6 composites, large cracks and a carbonation of PA6 was found on the exterior surface of Ultramid® B3WG7 sample, which led to an acceleration of diffusion of heat and oxygen. While the majority of carbon fibres were embedded in the PA6 resin, more glass fibres were exposed to air in glass fibre reinforced composites. Since fibres acted as a heat/oxygen diffusion stopper, the incorporation of carbon fibres favored a better thermo-oxidative stability during

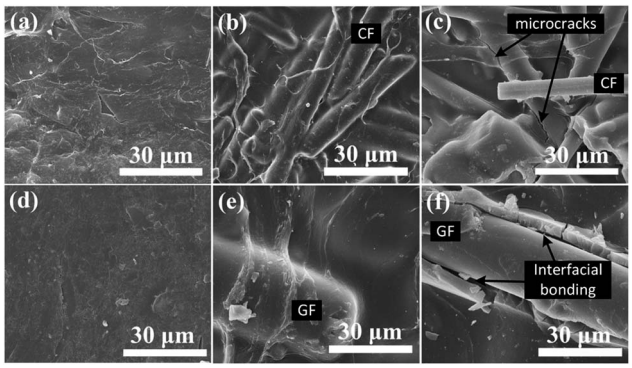

Fig. 9 SEM micrographs of surfaces of unaged CF/PA6 specimens aged at 180 °C for (a) 0 h, (b) 400 h, (c) 1600 h and Ultramid® B3WG7 specimen aged for (d) 0 h, (e) 400 h, (f) 1600 h.

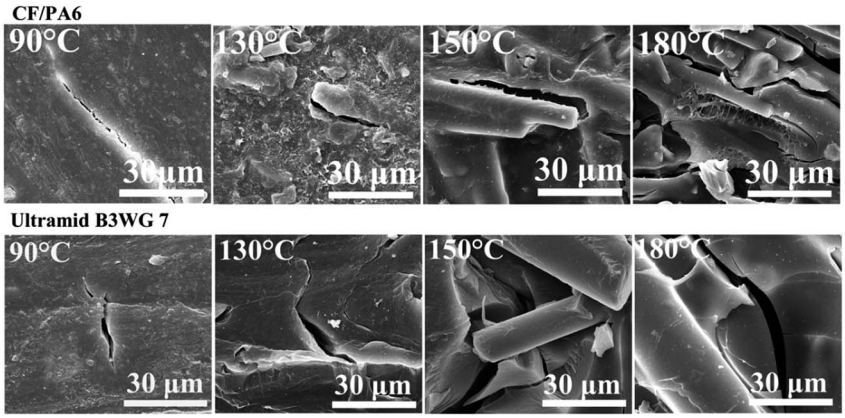

Fig. 10 SEM micrographs of surface microstructure of CF/PA6 and Ultramid® B3WG7 specimen at varying ageing temperatures for 1600 h.

the ageing process. The possible reasons for these observations may be due to a relative strong interfacial bonding between silane-treated carbon fibres and PA6 matrix.

In order to check the existence of color gradient along the sample thickness, composites at different ageing temperatures were cut-edged and the polished cross-sections were inspected. The processing steps of samples were according to schematic illustration in ESI (Fig. S3†). It is observed that the color gradient were only occurred in external surface of Ultramid® B3WG7 samples (as shown in ESI, Fig. S4†), and the color change was drastic with increasing ageing temperatures. To look deeper into the aged composites, the growth of oxidation layer was further investigated by metallurgic microscope, which was helpful to distinguish the transition from the oxidized layer to the un-oxidized zone.

As shown in metallographs (Fig. 11), the dark points were identified as the cross-section of glass fibres, and the surrounding bright area was attributed to the PA6 resin. Upon ageing, a superficial sub-layer was observed in aged specimens, which was characterized by an oxidized layer exposed to the thermo-oxidative ageing condition.[43] The thickness of oxidized layer was found to be related to the thermo-oxidative ageing temperatures. When aged at 130 °C, the oxidized layer was not noticeable during the whole thermo-oxidative ageing. When the ageing temperature increased to 150 °C, the oxidized layer became thicken as the ageing period prolonged to 800 h, and finally formed an evident oxidized boundary after 1600 h ageing time. However, it's worth noting that the oxidation zone at 180 °C was smaller than that at 150 °C. A reason for this phenomenon might be attributed to the massive loses of volatile degraded products took place in the ageing process at high temperature. Despite evident variation oxidized layer was observed in metallographs, the thermo-oxidative degradation of fibre reinforced PA6 composites was restricted to a very thin superficial layer, with only a thickness about 150 μm.

3.5 Thermo-oxidative ageing mechanisms

Based on the proposed thermo-oxidative ageing model, the ageing of composites can be accelerated by the temperature, oxygen concentration and the mechanical stresses. In our studies, the oxygen concentration were constant, therefore, the oxidation zone of CF/PA6 and Ultramid® B3WG7 composites were greatly dependent on the ageing temperatures. A schematic illustration of thermo-oxidative ageing mechanism of composite materials for varying ageing temperatures was presented in Fig. 12. When the composites exposed to thermo-oxidative ageing condition, an oxidation layer on the surface was formed, including the volatile and non-volatile products.

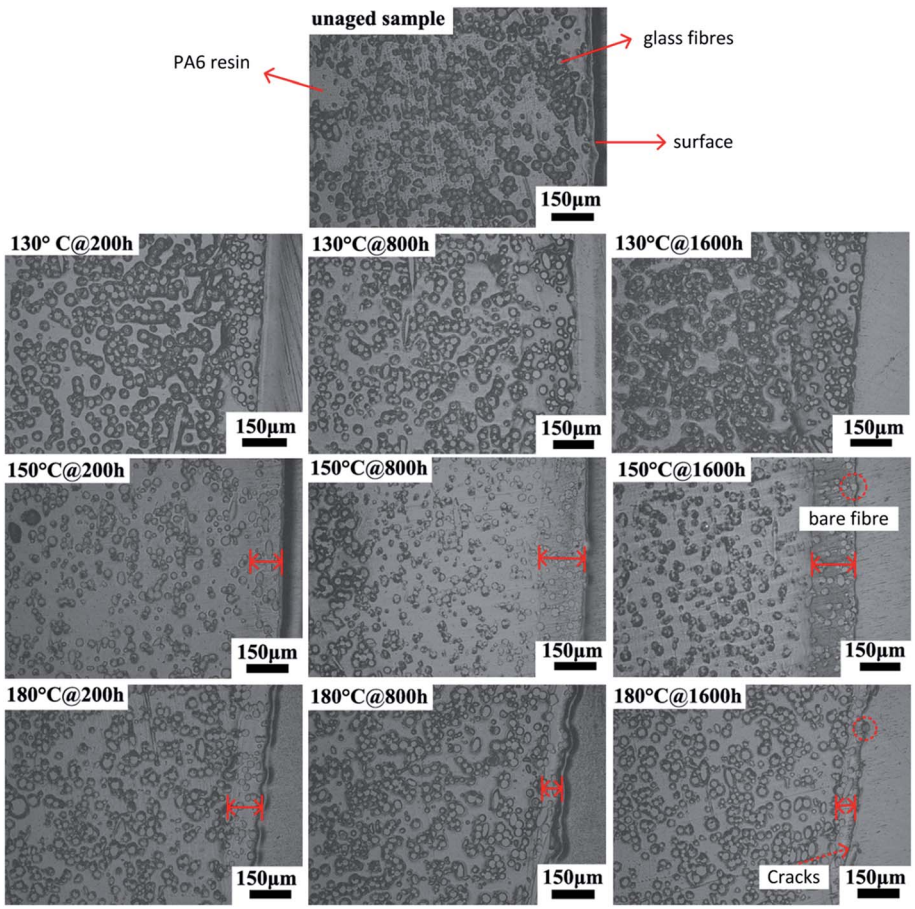

Fig. 11 Images of oxidization front growth in Ultramid® B3WG7 specimen at different ageing temperatures.

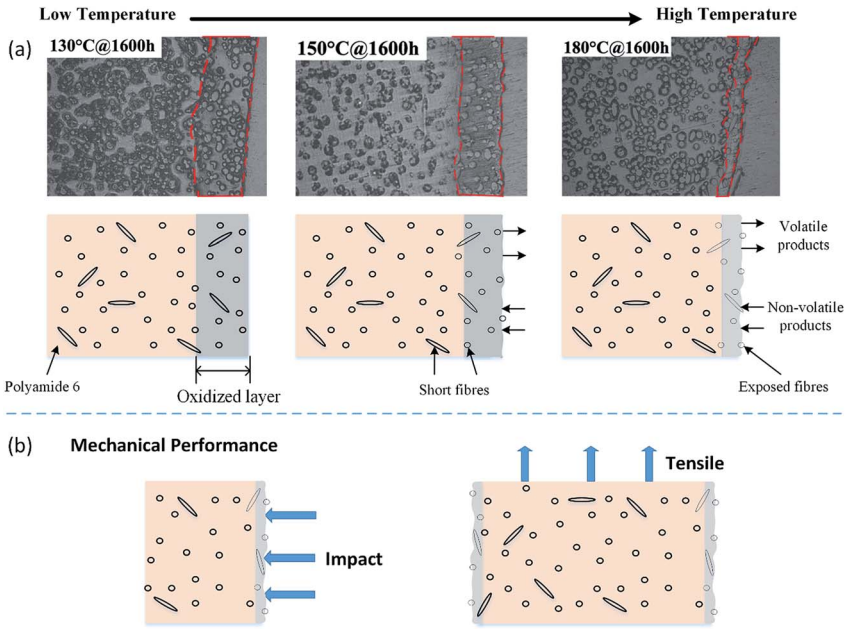

Fig. 12 Schematic model of mechanical performance of short fibre reinforced polyamide 6 composites for thermo-oxidation ageing for different ageing temperatures.

Accordingly, the surface oxidative layer acted as a barrier to prevent oxygen from penetrating deeper into the inner bulk of the composites, slowed down the volatilization of low-molecular-weight molecules, and thus protected the bulk PA6 from further oxidation. As the ageing continued, the scission of volatile products exceeded the formation of reactive zone, resulting in a decrease thickness of oxidized layer. However, the inner core of the composite material was not greatly affected during the whole ageing period, as illustrated by the metallographs (as shown in Fig. 11). Similar degradation mechanism has been proposed on polyimide thick specimens.[44,45]

Furthermore, the thermo-oxidative ageing mechanism was dependent on two initial parameters: the kinetic of the oxygen diffusion on the material bulk, and the kinetics of the oxygen reaction with PA6 molecular. For composite materials, incorporation of fibres and the fibre/matrix bonding strongly influenced the thermal and mechanical properties during thermo-oxidative ageing process.[46] When the composites were exposed to thermo-oxidation condition for a period, PA6 resin around the fibres degraded and generated small molecules, resulting in interfacial debonding between fibres and the matrix. Higher ageing temperature accelerated the volatilization of small molecules, which induced more cracks on the surface of composite samples (as revealed by SEM images, Fig. 9 and 10). In combination with mechanical test results, the impact strength of composite materials was greatly affected during the ageing process, which is probably due to the weakening of fibre/PA6 interfacial region and the embrittlement of PA6 matrix. With weaken fibre/matrix interface and more cracks on composite surface, the stress directly contacting the fibre surface, which can result in fibre fracture under a small load. However, the fibre/matrix interfacial region and PA6 matrix in composite bulk core were not affected under long-term thermo-oxidation, which could efficiently absorbed fracture energy along the tension direction. Consequently, it is expected that the well maintained interface adhesion between silane-treated carbon fibre and PA6 contributed to more excellent comprehensive ageing mechanical properties than Ultramid® B3WG7 specimen.

4. Conclusions

The aim of this study was to investigate the thermo-oxidative ageing effect on mechanical and morphology of short fibre reinforced polyamide 6 composites exposed to different exposure temperatures ranging from 90 to 180 °C for a long-time period of 1600 h. The ageing behavior of CF/PA6 and Ultramid® B3WG7 (glass fibres reinforced PA6) were comparatively investigated. For mechanical performance, it is revealed that a well-reserved retention of tensile strength for CF/PA6 composites was obtained at relatively high ageing temperatures, whereas the retention of tensile strength for Ultramid® B3WG7 samples were slightly declined after long-term thermo-oxidative exposure. Both CF/PA6 and Ultramid® B3WG7 composites showed continuously decrease in notched impact strength. An increase in T_g was observed in the initial ageing process, which may contribute to an increase in tensile strength for composite samples. However, as ageing time prolonged, a slightly decreased thermal stability of PA6 matrix (especially in Ultramid® B3WG7 sample) was observed in TGA curves. Evident color changes were observed in Ultramid® B3WG7 composites during ageing process. In FTIR spectroscopy, characteristics peaks of PA6 were reduced or disappeared, and chromophoric group (*i.e.* ketone) were formed, which explained the color transition of specimens. Furthermore, SEM investigations showed degradation of surface material at the fibre/

matrix interface, with change in surface texture and exposure of fibres of the aged composite materials. It is found that the matrix surface and interfacial debond were more seriously damaged in Ultramid® B3WG7 composites during the ageing process. The metallographs of polished cross-sectional samples presented changes of oxidized zone at varying ageing temperatures. A degradation mechanism was generated from the previous findings: the impact strength of fibre reinforced polyamide 6 composites was greatly affected by the superficial oxidized layer, while the tensile strength was more dependent on the main core of composites.

Conflicts of interest

There are no conflicts to declare.

Acknowledgements

This work was financially supported by China Postdoctoral Science Foundation (2015M571300), the Fundamental Research Funds for the Central Universities (DUT17RC(4)57).

References

1 K. Marchildon, *Macromol. React. Eng.*, 2011, **5**, 22–54.
2 X. Fu, B. He and X. Chen, *J. Reinf. Plast. Compos.*, 2010, **29**, 936–949.
3 F. Truckenmuller and H. G. Fritz, *Polym. Eng. Sci.*, 1991, **31**, 1316–1329.
4 W. Dong and P. Gijsman, *Polym. Degrad. Stab.*, 2010, **95**, 1054–1062.
5 E. Carlson and K. Nelson, *Automot. Eng.*, 1996, **104**, 84–89.
6 R. Bernstein, D. K. Derzon and K. T. Gillen, *Polym. Degrad. Stab.*, 2005, **88**, 480–488.
7 M. J. Clifford and T. Wan, *Polymer*, 2010, **51**, 535–539.
8 O. Meincke, D. Kaempfer, H. Weickmann, C. Friedrich, M. Vathauer and H. Warth, *Polymer*, 2004, **45**, 739–748.
9 A. Hassan, R. Yahya, A. H. Yahaya, A. Tahir and P. R. Hornsby, *J. Reinf. Plast. Compos.*, 2004, **23**, 969–986.
10 J. L. Thomason, *Polym. Compos.*, 2006, **27**, 552–562.
11 B. Mouhmid, A. Imad, N. Benseddiq and D. Lecompte, *Compos. Sci. Technol.*, 2009, **69**, 2521–2526.
12 J. L. Thomason, *Compos. Sci. Technol.*, 1999, **59**, 2315–2328.
13 A. Bernasconi, P. Davoli, A. Basile and A. Filippi, *Int. J. Fatigue*, 2007, **29**, 199–208.
14 M. K. Akkapeddi, *Polym. Compos.*, 2000, **21**, 576–585.
15 R. F. Li and X. Z. Hu, *Polym. Degrad. Stab.*, 1998, **62**, 523–528.
16 P. Cerruti and C. Carfagna, *Polym. Degrad. Stab.*, 2010, **95**, 2405–2412.
17 T. Mazan, R. Berggren, J. K. Jorgensen and A. Echtermeyer, *J. Appl. Polym. Sci.*, 2015, **132**, 6249–6260.
18 J. L. Thomason, J. Z. Ali and J. Anderson, *Composites, Part A*, 2010, **41**, 820–826.
19 N. Y. Jia, H. A. Fraenkel and V. A. Kagan, *J. Reinf. Plast. Compos.*, 2004, **23**, 729–737.
20 F. Dan and T. Bjorn, *Polym. Degrad. Stab.*, 2000, **67**, 69–78.
21 Y. Shu, L. Ye and T. Yang, *J. Appl. Polym. Sci.*, 2008, **110**, 945–957.
22 C. H. Do, E. M. Pearce, B. J. Bulkin and H. K. Reimschuessel, *J. Polym. Sci., Part A: Polym. Chem.*, 1987, **25**, 2409–2424.
23 A. T. Hagler and A. Lapiccirella, *Biopolymers*, 1976, **15**, 1167–1200.
24 J. Koen, G. Pieter and T. Daan, *Polym. Degrad. Stab.*, 1995, **49**, 127–133.
25 G. Pieter, T. Daan and J. Koen, *Polym. Degrad. Stab.*, 1995, **49**, 121–125.
26 H. Song, D. Zhou and J. Guo, *Polym. Compos.*, 2016, DOI: 10.1002/pc.24174.
27 X. Zuo, H. Shao, D. Zhang, Z. Hao and J. Guo, *Polym. Degrad. Stab.*, 2013, **98**, 2774–2783.
28 B. Lánská, *Eur. Polym. J.*, 1994, **30**, 197–204.
29 L. Sang, Y. K. Wang, G. Y. Chen, J. C. Liang and Z. Y. Wei, *RSC Adv.*, 2016, **6**, 107739–107747.
30 C. Zhang, H. Wu and M. R. Kessler, *Polymer*, 2015, **69**, 52–57.
31 I. Ksouri, N. Guermazi, N. Haddar and H. F. Ayedi, *Polym. Compos.*, 2016, DOI: 10.1002/pc.23961.
32 L. U. Devi, S. S. Bhagawan and S. Thomas, *Polym. Compos.*, 2011, **32**, 1741–1750.
33 M. A. Sawpan, P. G. Holdsworth and P. Renshaw, *Mater. Des.*, 2012, **42**, 272–278.
34 S. R. Patel and S. W. Case, *Int. J. Fatigue*, 2002, **24**, 1295–1301.
35 M. Perera, U. S. Ishiaku and Z. Ishak, *Polym. Degrad. Stab.*, 2000, **68**, 393–402.
36 X. Wang, H. Yang, L. Song, Y. Hu, W. Xing and H. Lu, *Compos. Sci. Technol.*, 2011, **72**, 1–6.
37 J. C. Liang, C. Ding, Z. Y. Wei, L. Sang, P. Song, G. Y. Chen, Y. Chang, J. T. Xu and W. X. Zhang, *Polym. Compos.*, 2015, **36**, 1335–1345.
38 W. Fan, J. Li, Y. Zheng, T. Liu, X. Tian and R. Sun, *Polym. Degrad. Stab.*, 2016, **123**, 162–169.
39 D. Flore, K. Wegener, D. Seel, C. C. Oetting and T. Bublat, *Composites, Part A*, 2016, **90**, 359–370.
40 C. H. Do, E. M. Pearce, B. J. Bulkin and H. K. Reimschuessel, *J. Polym. Sci., Part A: Polym. Chem.*, 1986, **24**, 1657–1674.
41 S. Ohno, M. H. Lee, K. Y. Lin and F. S. Ohuchi, *Mater. Sci. Eng., A*, 2000, **293**, 88–94.
42 G. Schoeppner, G. Tandon and E. Ripberger, *Composites, Part A*, 2007, **38**, 890–904.
43 P. Cerruti, C. Carfagna, J. Rychly and L. Matisova-Rychla, *Polym. Degrad. Stab.*, 2003, **82**, 477–485.
44 M. Meador, C. E. Lowell, P. J. Cavano and P. HerreraFierro, *High Perform. Polym.*, 1996, **8**, 363–379.
45 R. Khazaka, M. L. Locatelli, S. Diaham and P. Bidan, *Polym. Degrad. Stab.*, 2013, **98**, 361–367.
46 M. P. Foulc, A. Bergeret, L. Ferry, P. Ienny and A. Crespy, *Polym. Degrad. Stab.*, 2005, **89**, 461–470.

